

# Nomograms for maximum pressure angles in radial cams with follower eccentricity for cycloidal and harmonic motion curves

Artur Henrique de Freitas Avelar\* and Luiza Fernandes Soares

Departamento de Engenharia Mecânica, Universidade Federal de São João del Rei, Praça Frei Orlando, 170, 36307-352, São João del Rei, Minas Gerais, Brazil. \*Author for correspondence. E-mail: arturavelar@ufsj.edu.br

**ABSTRACT.** For an adequate design of radial cams with translating roller followers, it is necessary to maintain the constraint that maximum pressure angle cannot exceed the empirically accepted value of  $30^\circ$ . The direct calculation of this parameter is difficult and it is usually sought to reduce it by trial and error. Nomograms that exist so far only calculated this angle for cams with no eccentricity between follower and cam. This research presents two nomograms with this additional parameter, which allows for greater design freedom using all available variables. The charts are for cycloidal and harmonic motion curves, and can be used for their full and half curves. The study discusses the advantages of using nomograms and the methods to obtain low values of maximum pressure angle by satisfactorily combining available parameters. Although nomograms are no longer a widely used tool in the industry, they still have didactic functions in textbooks and could be useful for preliminary analysis in engineering projects.

**Keywords:** Planar mechanisms; cams; pressure angle; eccentricity; nomogram.

Received on February 15, 2021.

Accepted on March 29, 2022.

## Introduction

Radial cam mechanisms with translating roller followers have as a constraint the pressure angle  $\alpha$ , that is, the angle between the line of action and the centerline of the follower (Figure 1). The maximum pressure angle value  $\alpha_{\max}$  during a full rotation is accepted empirically as  $30^\circ$  (Rothbart, 2004; Norton, 2012), however, there are cases in particular conditions where angles up to  $48^\circ$  did not interfere with the mechanism's movement (Rothbart, 2004).

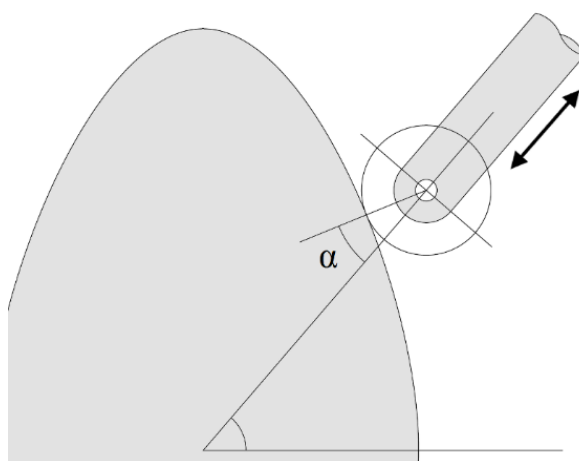


**Figure 1.** Section of a radial cam with a translating roller follower showing pressure angle  $\alpha$  that the roller makes with cam surface at the contact point.

There are several methods for controlling maximum pressure angle. Norton (2012; 2009) makes use of trial and error and use the eccentricity between the follower axis of motion and the cam rotation axis to reduce the maximum value, where a positive eccentricity value may reduce pressure angle on follower rise, but it will increase it on follower return. Recent methods make use of parametric polynomials and optimization tools to maintain pressure angle at established limits (Rothbart, 2004, Farouki & Manjunathaiah, 1998; Flores, 2013; Yu & Lee, 1998).

The use of nomograms was very common in engineering for quickly making complex calculations, and, although they fell into disuse due to increasing use of calculators and computers, they can still be found in recent publications in various engineering fields (Bagaria, Doerfler, & Roschier, 2017; Esmail, Pennestrib, & Juber, 2018; Hwang & Chen, 2007; Ma, Chong, & Liao, 2020). Nomograms are tools that have the advantages of being simple and quick to apply, in addition to being a graphical representation of the problem as a whole, providing a valuable insight into the relationship between the input parameters. These charts acquire a new significance when used as a didactic tool for undergraduate students learning complex mechanical design problems through a simple and fast resolution method.

Varnum (1951) created the first nomogram for maximum pressure angle on cams for cycloidal motion and constant acceleration curves. Subsequently, the chart was expanded to the harmonic and 8th order polynomial curves (Mabie & Reinholtz 1987) and is widely used in current textbooks (Rao, 2011; Ambekar, 2007; Dicker, Pennock, & Shigley, 2003). However, the nomogram can only be properly used in the particular case where there is no eccentricity between follower and axis of rotation of the cam. The only results for maximum pressure angle with eccentricity are from Jensen (1987), which can only be used when follower rise and return have the same motion curve, and Suchora, Werner, and Paine (1994), in which a different chart is required for each eccentricity value.

The objective of this study is to create nomograms for the general case of translating follower eccentricity for cycloidal and harmonic movement curves for direct calculation of the maximum pressure angle. Nomograms can be used for full curves and a method for using half curves is presented.

## Material and methods

Figure 2 illustrates the nomenclature used for cams, where  $R'$  is the distance of the cam from the rotation center to the roller follower center;  $R$  is the base radius;  $\varepsilon$  is the eccentricity, that is, the perpendicular distance between the movement axis of the follower and the rotation center of the cam;  $L$  is the stroke and  $\theta$  is the rotation angle of the cam.

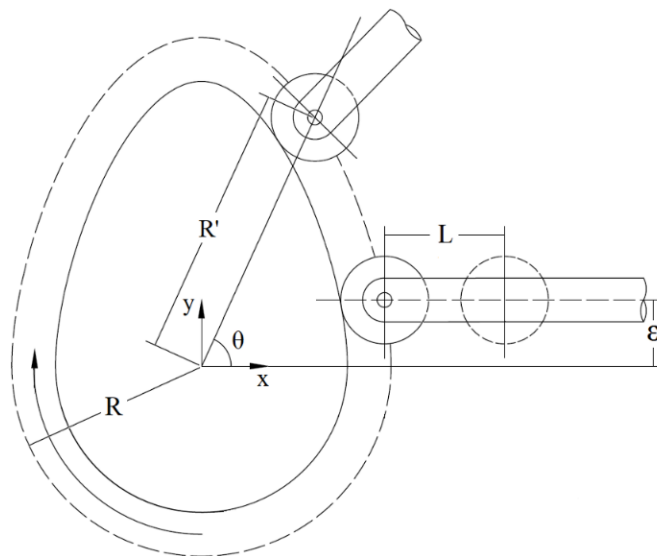


**Figure 2.** Cam nomenclature.  $R'$  - distance of the cam from the rotation center to the roller follower center;  $R$  - base radius;  $\varepsilon$  - eccentricity,  $L$  - follower stroke;  $\theta$  - rotation angle of the cam.

Eccentricity can have positive and negative values, which influence the pressure angle. For a cam with clockwise rotation, eccentricity will be considered positive when it is in the positive direction of the  $y$ -axis (Figure 2).

Figure 3 shows cycloidal and harmonic motion curves, along with their half curves, with respective formulas for displacement  $S$  and velocity  $V$ . Equations show their relationship with  $L$ ,  $\theta$  and active cam angle  $\beta$ .

The general formula for calculating pressure angle with eccentricity of the follower is shown in Equation (1). Values for displacement and velocity depend on the chosen motion curve.

$$\tan(\alpha) = \frac{V - \varepsilon}{S + \sqrt{R^2 - \varepsilon^2}} \quad (1)$$

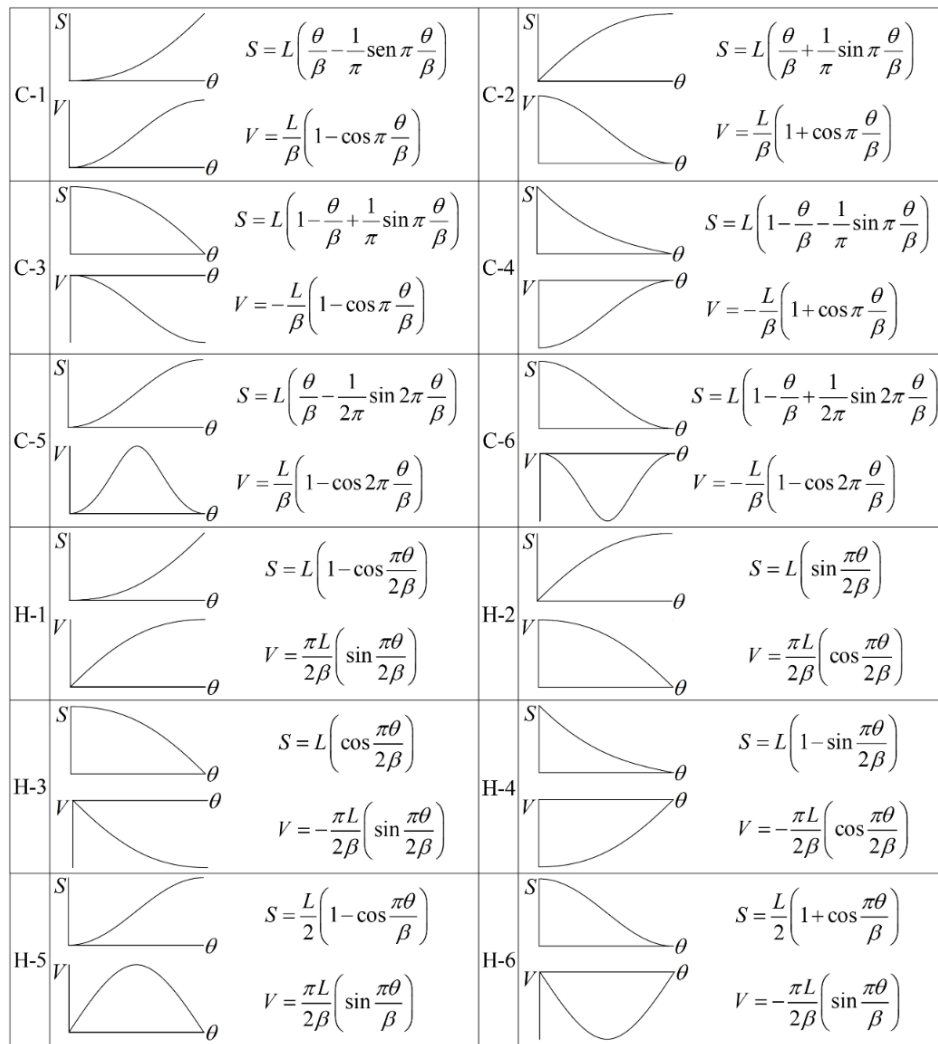


**Figure 3.** Cycloidal and harmonic displacement and velocity curves. Curves C-1 to C-4 are half-cycloidal curves for rise and return. Curves C-5 and C-6 are full cycloidal curves. Curves H-1 to H-4 are half-harmonic curves for rise and return. Curves H-5 and H-6 are full harmonic curves.

To find the maximum values of pressure angle, it is possible to differentiate this equation with respect to the rotation angle of the cam and equate it to zero, thus finding the values of the rotation angle  $\theta$  that yield the maximum and minimum pressure angles. There are resolutions for the equation for the case without eccentricity (Varnum, 1951), but the general case usually has an additional difficulty for producing terms without analytical solution. Therefore, for a rapid calculation, a nomogram is very effective.

The difference in results for follower rise or return is that pressure angle is positive for rise and negative for return. Using absolute values, it is possible to apply the same equations for both curves. A similar thing occurs when using positive and negative eccentricity values. A positive eccentricity in follower rise gives the same absolute maximum pressure angle as a negative eccentricity in a follower return movement.

### Cycloidal curves

Using the C-5 curve, Equation (1) is rewritten as:

$$\tan(\alpha) = \frac{\frac{L}{\beta} \left[ 1 - \cos \left( \frac{2\pi\theta}{\beta} \right) \right] - \varepsilon}{L \left[ \left( \frac{\theta}{\beta} \right) - \left( \frac{1}{2\pi} \right) \sin \left( \frac{2\pi\theta}{\beta} \right) \right] + \sqrt{R^2 - \varepsilon^2}} \quad (2)$$

We can take a similar approach as Varnum (1951) and differentiate the term directly from the tangent because it represents the slope of the curve. Thus, Equation (2) is differentiated and set equal to zero.

$$\frac{d \tan(\alpha)}{d\theta} = \frac{8\pi^2 \frac{L}{\beta} \sin\left(\frac{\pi\theta}{\beta}\right) \left[ 2\pi \cos\left(\frac{\pi\theta}{\beta}\right) (\theta L + \beta \sqrt{R^2 - \varepsilon^2}) + \beta \sin\left(\frac{\pi\theta}{\beta}\right) (\beta\varepsilon - 2L) \right]}{\left[ \beta L \sin\left(\frac{\pi\theta}{\beta}\right) - 2\pi (\theta L + \beta \sqrt{R^2 - \varepsilon^2}) \right]^2} = 0 \quad (3)$$

After simplifications, it results in:

$$2\pi \cos\left(\frac{\pi\theta}{\beta}\right) (\theta L + \beta \sqrt{R^2 - \varepsilon^2}) + \beta \sin\left(\frac{\pi\theta}{\beta}\right) (\beta\varepsilon - 2L) = 0 \quad (4)$$

Following Varnum's (1951) methodology, by letting  $\pi\theta/\beta$  equal an auxiliary angle B, Equation (4) reduces to:

$$2L [\tan(B) - B] - \beta\varepsilon \tan(B) - 2\pi \sqrt{R^2 - \varepsilon^2} = 0 \quad (5)$$

Equation (5) does not have an analytical solution for B, being necessary the use of a numerical or graphical method for its proper resolution. Thus, a nomogram will be created to obtain the value of B.

Equation (5) is only true for calculating the maximum pressure angle. Therefore, by substituting it back into Equation (2) and simplifying, Equation (2) can be reduced to:

$$\tan(\alpha_{\max}) = \frac{2\pi}{\beta} \cot(B) \quad (6)$$

### Harmonic curves

Using the H-5 curve, Equation (1) is rewritten as:

$$\tan(\alpha) = \frac{\frac{\pi L}{2\beta} \sin\left(\frac{\pi\theta}{\beta}\right) - \varepsilon}{\frac{L}{2} \left[ 1 - \cos\left(\frac{\pi\theta}{\beta}\right) \right] + \sqrt{R^2 - \varepsilon^2}} \quad (7)$$

We differentiate the term directly from the tangent because it represents the slope of the curve. Thus, Equation (7) is differentiated and set equal to zero.

$$\frac{d \tan(\alpha)}{d\theta} = \frac{\frac{\pi L}{\beta} \left[ \pi \cos\left(\frac{\pi\theta}{\beta}\right) (L + 2\sqrt{R^2 - \varepsilon^2}) + 2\beta\varepsilon \sin\left(\frac{\pi\theta}{\beta}\right) - \pi L \right]}{\beta \left\{ L \left[ 1 - \cos\left(\frac{\pi\theta}{\beta}\right) \right] + 2\sqrt{R^2 - \varepsilon^2} \right\}^2} = 0 \quad (8)$$

After simplifications, it results in:

$$\pi \cos\left(\frac{\pi\theta}{\beta}\right) (L + 2\sqrt{R^2 - \varepsilon^2}) + 2\beta\varepsilon \sin\left(\frac{\pi\theta}{\beta}\right) - \pi L = 0 \quad (9)$$

By letting  $\pi\theta/\beta$  equal an auxiliary angle B, Equation (9) reduces to:

$$\pi L \left[ \frac{1 - \cos(B)}{\cos(B)} \right] - 2\beta\varepsilon \tan(B) - 2\pi \sqrt{R^2 - \varepsilon^2} = 0 \quad (10)$$

Again, Equation (10) has no analytical solution for B, requiring the use of a numerical or graphical method for its proper resolution. Thus, a nomogram will be created to obtain the value of B.

Equation (10) is only true for calculating the maximum pressure angle. Therefore, by substituting it back into Equation (7) and simplifying, Equation (7) can be reduced to:

$$\tan(\alpha_{\max}) = \frac{\pi}{\beta} \cot(B) \quad (11)$$

### Nomography

One method to plot nomograms is using parametric equations. Equation (12) shows a standard nomographic form using a determinant notation. To plot it, all axes have to be on the same plane, implying a linear dependence on the columns of the matrix, thus its determinant equals zero. In an equation with variables  $u$ ,  $v$  and  $w$ , the  $u$ -scale is plotted by parametric functions in the first row, where functions  $x(u)$  and  $y(u)$  are used to calculate the  $(x, y)$ -coordinate for each value of  $u$  on the scale. The third column is unitary because the nomogram is plotted on a plane (Doerfler, 2009; Epstein, 1958).

$$\det \begin{bmatrix} x(u) & y(u) & 1 \\ x(v) & y(v) & 1 \\ x(w) & y(w) & 1 \end{bmatrix} = 0 \quad (12)$$

A single nomogram for an equation of 4 to 6 variables can still be created if the determinant in standard nomographic form contains functions of no more than two variables per row. The single scale for a one-variable row is replaced by a grid of scales for values of each of the two variables, resulting in a grid nomogram (Doerfler, 2009; Epstein, 1958).

### Nomograms for cycloidal curves

For the cycloidal curve, we will make a compound nomogram, the first part solves Equation (5) and the next solves Equation (6).

Equation (5) can be written in matrix form as:

$$\det \begin{bmatrix} \tan(B) & 2\pi\sqrt{R^2 - \varepsilon^2} & \tan(B) - B \\ 1 & -\beta\varepsilon & 0 \\ 0 & 2L & 1 \end{bmatrix} = 0 \quad (13)$$

One can manipulate Equation (13) in several ways, not changing its determinant, to bring it into standard nomographic form. Each will create a different nomogram. Equation (12) and (13) show two different configurations.

$$\det \begin{bmatrix} \frac{-\varepsilon \tan(B)}{(1-\varepsilon)\tan(B)-B} & \frac{\pi\sqrt{R^2 - \varepsilon^2}}{(1-\varepsilon)\tan(B)-B} & 1 \\ 1 & \frac{\beta}{2} & 1 \\ 0 & L & 1 \end{bmatrix} = 0 \quad (14)$$

$$\det \begin{bmatrix} \frac{\varepsilon \tan(B)}{(1+\varepsilon)\tan(B)-B} & \frac{\pi\sqrt{R^2 - \varepsilon^2}}{(1+\varepsilon)\tan(B)-B} & 1 \\ 1 & -\frac{\beta}{2} & 1 \\ 0 & L & 1 \end{bmatrix} = 0 \quad (15)$$

As previously stated, one row cannot contain more than two variables. In order to keep this true, we can assign ratios  $M = L/R$  and  $N = \varepsilon/R$  to Equation (5) and rewrite the previous matrices as:

$$\det \begin{bmatrix} \frac{-N \tan(B)}{(1-N) \tan(B) - B} & \frac{\pi \sqrt{1-N^2}}{(1-N) \tan(B) - B} & 1 \\ 1 & \frac{\beta}{2} & 1 \\ 0 & M & 1 \end{bmatrix} = 0 \quad (16)$$

$$\det \begin{bmatrix} \frac{N \tan(B)}{(1+N) \tan(B) - B} & \frac{\pi \sqrt{1-N^2}}{(1+N) \tan(B) - B} & 1 \\ 1 & -\frac{\beta}{2} & 1 \\ 0 & M & 1 \end{bmatrix} = 0 \quad (17)$$

When analyzing the second row, it can be seen that the x-coordinate will always be 1 while variable  $\beta$  will be plotted in a vertical scale along y-coordinates according to its function. The same happens with  $M$ , where it will be plotted at  $x = 0$ . Variables  $B$  and  $N$  will be plotted as a grid in a curved scale.

To create the charts, the PyNomo package available for Python was used. The respective nomograms for Equations (16) and (17) are shown in Figure 4.

The  $B$  and  $L/R$  scales were adjusted to optimize the nomograms. Variable  $B$ , being in a tangent function, varies from  $0^\circ$  to  $90^\circ$  ( $\pi/2$  rad), however, values greater than 1.5 make the grid too crowded, hindering its visualization, also values lower than 1.0 expand the grid in a geometric progression, which hinders visualization of some values of other variables; moreover, low values of  $B$  seem to be useful only for higher  $L/R$  ratios. Thus, the limits for  $B$  ranged from 1.0 to 1.5 and for  $L/R$  ranged from 0 to 5. Ratio  $\varepsilon/R$  ranges from 0, where there is no eccentricity, to 1, the maximum possible eccentricity to still maintain contact between follower and cam. Active cam angle  $\beta$  ranges from  $0^\circ$  to the extreme value of full rotation of  $360^\circ$ .

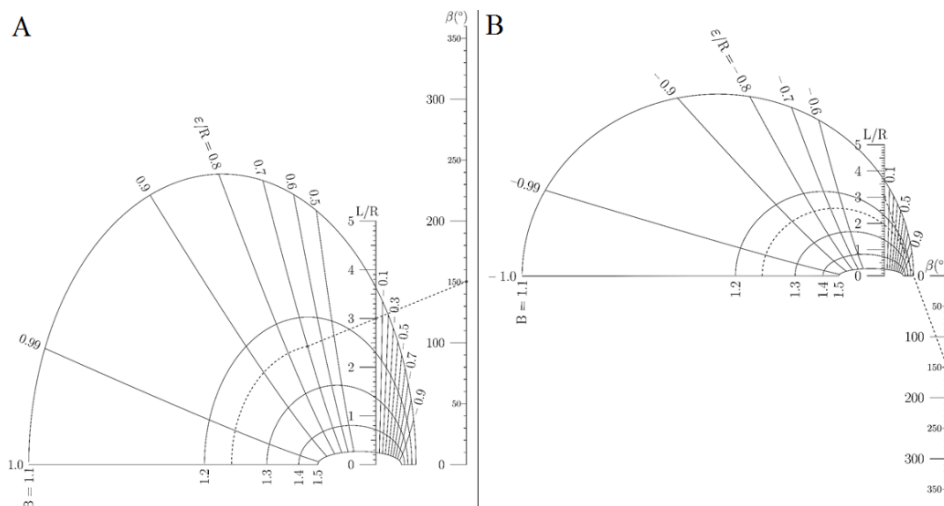


**Figure 4.** Nomograms for finding  $B$  for cycloidal curve. (A) Nomogram for Equation (16), (B) Nomogram for Equation (17).

The nomograms in Figure 4 have a dashed line, called isopleth, which shows a generic example on how to use the nomogram. In this example, we have  $L/R = 3$ ,  $\beta = 150^\circ$  and  $\varepsilon/R = 0.7$ . We need to connect these three values to find the correct answer for  $B$ . All we need to do is draw a straight line between values of  $L/R$  and  $\beta$ , and find where the isopleth crosses the line of  $\varepsilon/R = 0.7$ . Next, we follow along the grid curve to its edge and find a value of  $B = 1.24$ . Both charts give the same answer for this example.

Figure 4(A) does not have good visibility for negative  $\varepsilon/R$  values, this can provide  $B$  values with poor accuracy. At the same time, Figure 4(B) shows a small  $L/R$  scale, in addition to a large and useless blank space. In order to create an optimized chart, only the section of negative  $\varepsilon/R$  values in Figure 4(A) was used and only

the section of positive  $\varepsilon/R$  values in Figure 4(B). By rotating  $\beta$  axis in Figure 4(A) and aligning it with the same axis in Figure 4(B), it is possible to create a nomogram for Equation (5) with good visibility for positive and negative  $\varepsilon/R$  values. Its size is adjusted for better visualization (Figure 5). Note that  $L/R$  axis is positive in either direction and  $\varepsilon/R = 1$  and  $-1$  are the same point.

Next, for Equation (6), first we have to use logarithmic properties to represent it as additions:

$$\log(\beta) - \{\log(2\pi) + \log[\cot(B)]\} + \log[\tan(\alpha_{\max})] = 0 \quad (18)$$

Then, it is possible to create a matrix for the above equation.

$$\det \begin{bmatrix} -1 & \log(\beta) & 1 \\ 0 & 0.5\{\log(2\pi) + \log[\cot(B)]\} & 1 \\ 1 & \log[\tan(\alpha_{\max})] & 1 \end{bmatrix} = 0 \quad (19)$$

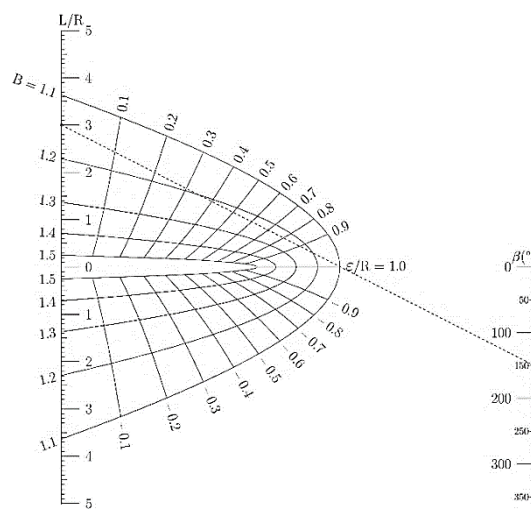


Figure 5. Final nomogram for finding B for cycloidal curve.

Its respective nomogram can be seen in Figure 6.

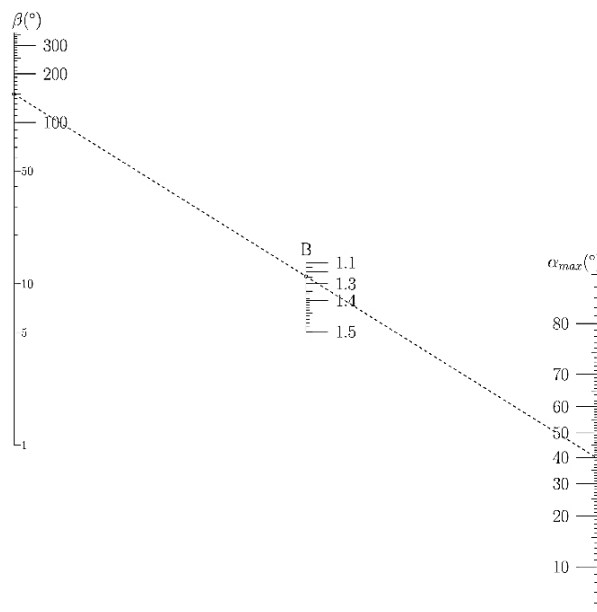


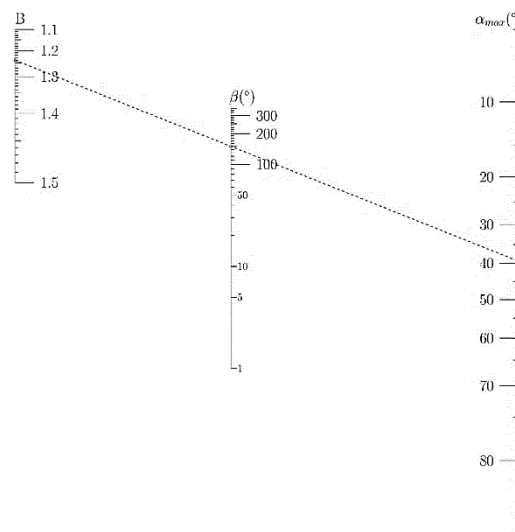
Figure 6. Nomogram for maximum pressure angle for cycloidal curve.

Figure 6 has an issue that the  $B$  axis is small and located in between the other two scales, making it impossible to join the two nomograms into one. However, it is possible to apply a transformation tool called

projection to modify the chart. Epstein (1958) explains that, by choosing a point in the coordinates of the nomogram and using it as a center of perspective, it is possible to project the original chart on another plane and modify its appearance without losing the equation's nomographic properties. Equation (20) shows the procedure that must be done to use the projection transformation, where  $x_p$ ,  $y_p$  and  $z_p$  are the points in the center of perspective.

$$\begin{bmatrix} x(u) & y(u) & 1 \\ x(v) & y(v) & 1 \\ x(w) & y(w) & 1 \end{bmatrix} \cdot \begin{bmatrix} z_p & y_p & 1 \\ 0 & -x_p & 1 \\ 0 & 0 & -x_p \end{bmatrix} \quad (20)$$

Choosing points  $x_p = 0.4$ ,  $y_p = 0.25$  and  $z_p = 1.0$ , we arrive at Figure 7. It relocates B axis to make it easier to join the nomograms.  $\alpha_{\max}$  was set to range from  $5^\circ$  to  $85^\circ$ ; values close to  $0^\circ$  and  $90^\circ$  tend to infinity due to the logarithmic and tangent terms, respectively, as can be seen as the scale stretches close to these limits.



**Figure 7.** Nomogram for maximum pressure angle for cycloidal curve after projection transformation.

The isopleth shows the continuation of the generic example. We take  $B = 1.24$  and  $\beta = 150^\circ$ ; by joining these points in a straight line, we arrive at the approximate value of the maximum pressure angle  $\alpha_{\max} = 39.5^\circ$ .

### Nomograms for harmonic curves

For the harmonic motion curve, the same procedure is done. Equation (10) can be written in matrix form as:

$$\det \begin{bmatrix} 2 \tan(B) & 2\pi\sqrt{R^2 - \varepsilon^2} & \frac{1 - \cos(B)}{\cos(B)} \\ 1 & -\beta\varepsilon & 0 \\ 0 & \pi L & 1 \end{bmatrix} = 0 \quad (21)$$

The two configurations, where  $M = L/R$  and  $N = \varepsilon/R$ , used for the first part of the nomogram are:

$$\det \begin{bmatrix} \frac{-2N \sin(B)}{1 - \cos(B) - 2N \sin(B)} & \frac{\pi\sqrt{1 - N^2} \cos(B)}{1 - \cos(B) - 2N \sin(B)} & 1 \\ 1 & \frac{\beta}{2} & 1 \\ 0 & \frac{\pi M}{2} & 1 \end{bmatrix} = 0 \quad (22)$$



$$\det \begin{bmatrix} \frac{2N \sin(B)}{1 - \cos(B) + 2N \sin(B)} & \frac{\pi \sqrt{1 - N^2} \cos(B)}{1 - \cos(B) + 2N \sin(B)} & 1 \\ 1 & -\frac{\beta}{2} & 1 \\ 0 & \frac{\pi M}{2} & 1 \end{bmatrix} = 0 \quad (23)$$

Using only the section with negative  $\varepsilon/R$  values of Equation (22) and the section with positive  $\varepsilon/R$  values of Equation (23) and aligning the  $\beta$  axes of both, we arrive at the nomogram for finding  $B$  (Figure 8).

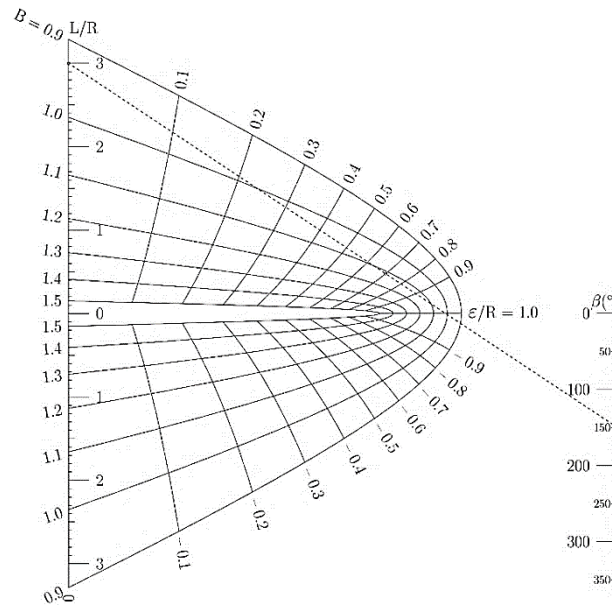


Figure 8. Final nomogram for finding  $B$  for harmonic curve.

Using the same previous generic example, values of  $L/R = 3$ ,  $\varepsilon/R = 0.7$  and  $\beta = 150^\circ$ , we find  $B = 1.11$ .

Next, Equation (11), with logarithmic properties, can be represented as:

$$\log(\beta) - \{\log(\pi) + \log[\cot(B)]\} + \log[\tan(\alpha_{\max})] = 0 \quad (24)$$

Its respective matrix can be written as:

$$\det \begin{bmatrix} -1 & \log(\beta) & 1 \\ 0 & 0.5\{\log(\pi) + \log[\cot(B)]\} & 1 \\ 1 & \log[\tan(\alpha_{\max})] & 1 \end{bmatrix} = 0 \quad (25)$$

Finally, after choosing projection points of  $x_p = 0.4$ ,  $y_p = 0.15$  and  $z_p = 1.0$ , its respective nomogram is seen in Figure 9. Using the same input values, for a  $B = 1.1$ , we have  $\alpha_{\max} = 30.5^\circ$ .

### Using nomograms for half curves

We can use the nomograms of full curves for half curves. The following method is based on the one of Kloomok and Muffley (1955), for nomograms without eccentricity.

Since the pressure angle chart is based on full curves, certain parameters of active cam angle and rise or return should be doubled for half curves in order to extend its boundaries. Extra care has to be taken on the use of second half rise curves and first half return curves (C-2, C-3, H-2, H-3), because the stroke must be subtracted from the base radius to have a zero initial displacement. Equations (26) to (30) sum up the procedure, where notation 0 means half curve parameters and notation 1 means the values to be used in the full curve nomograms.

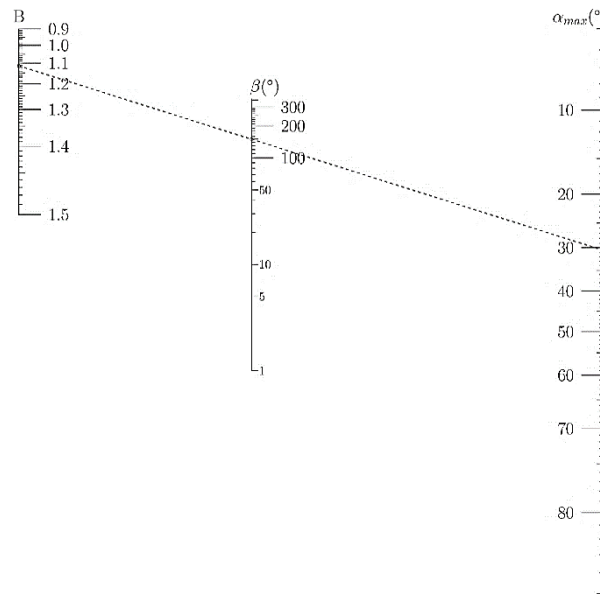


**Figure 9.** Nomogram for maximum pressure angle for harmonic curve after projection transformation.

$$L_1 = 2L_0 \quad (26)$$

$$\beta_1 = 2\beta_0 \quad (27)$$

$$\varepsilon_1 = \varepsilon_0 \quad (28)$$

$$R_1 = R_0 \quad (\text{for curves C-1, C-4, H-1, H-4}) \quad (29)$$

$$R_1 = R_0 - L_0 \quad (\text{for curves C-2, C-3, H-2, H-3}) \quad (30)$$

## Results and discussion

We can join the two separate charts to create a single compound nomogram for the full curves (Figures 10 and 11). The left side was mirrored for a better fit. As the B axes have different scales, a ladder nomogram, that is, an intermediate nomogram, is necessary for proper adjustment. We decided to use L/R ratio up to 3.0 to make a more compact chart.

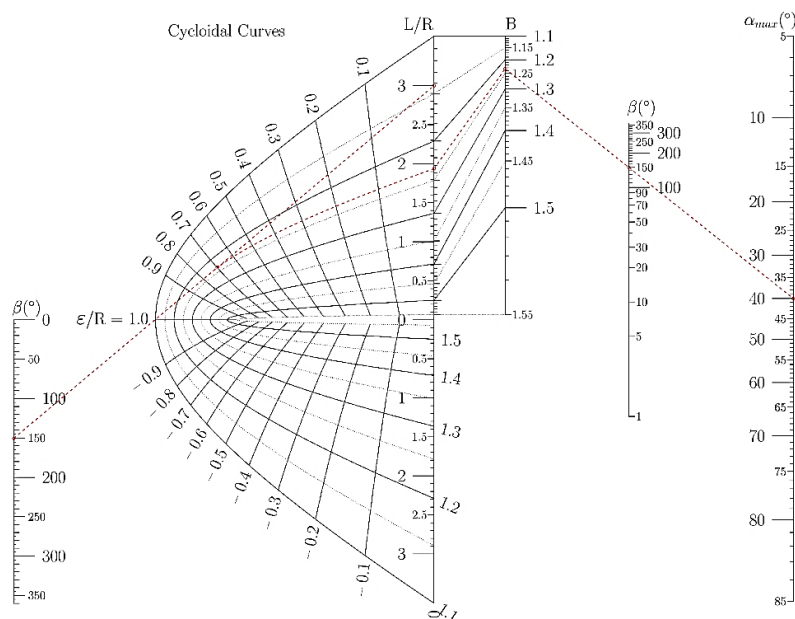


**Figure 10.** Final nomogram for cycloidal curve.

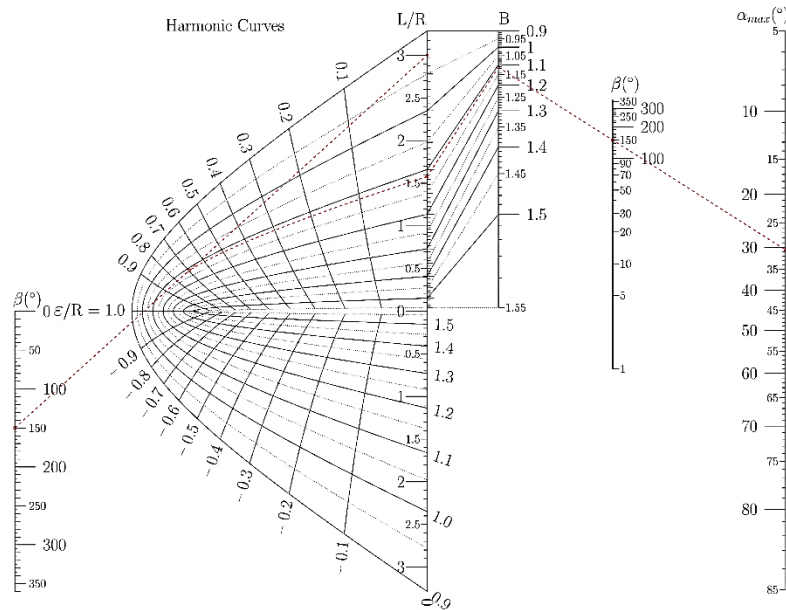


Figure 11. Final nomogram for harmonic curve.

To satisfactorily use the nomogram, a complete set of instructions follows. First, you connect points of  $L/R$  and  $\beta$  and check the point at which will cross the proper  $\varepsilon/R$  line. Next, follow the grid curvature to find the proper value of  $B$ . For the ladder nomogram, just get matching values for  $B$ . Finally, join  $B$  to the same previous value for  $\beta$  to find the maximum pressure angle  $\alpha_{\max}$ . It is imperative that the same  $\beta$  is used both times for the nomogram to work properly.

### Numerical examples and validation

Nomogram validation will be performed with two examples.

Example 1. A radial cam rotates clockwise, with  $R = 100$  mm,  $\varepsilon = +20$  mm, similar to Figure 2. Its displacement is illustrated in Figure 12 with one rise and one return; motion curves chosen were H-5 and H-6, respectively.

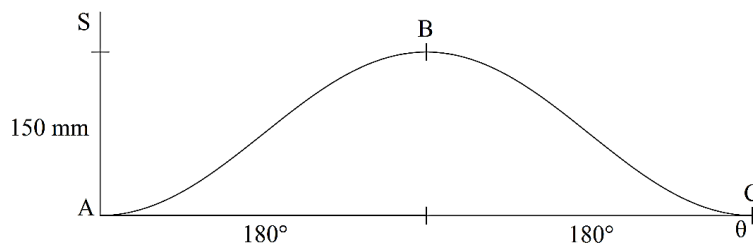


Figure 12. Displacement curve for Example 1.

For the first section, we have  $L/R = 150/100 = 1.5$ ;  $\varepsilon/R = 20/100 = 0.2$ ;  $\beta = 180^\circ$ . By looking at the left side of Figure 11, and using the three variables, we find a value of  $B = 1.24$ . Using this answer on the right side of the nomogram, along with the same value of  $\beta$ , we get an approximate maximum pressure angle  $\alpha_{\max} = 18.5^\circ$ .

For the second section, we have the same  $L/R$  and  $\beta$ , but, as discussed in topic 2, since it is a return motion, we have to use a negative value for eccentricity, thus  $\varepsilon/R = -20/100 = -0.2$ . By looking at the left side of Figure 11, we now find a value of  $B = 1.01$ . Using this answer on the right side, we get an approximate maximum pressure angle  $\alpha_{\max} = 32.0^\circ$ .

Plotting Equation (1) with these parameters, Figure 13 shows that maximum pressure angles for follower rise and return are, respectively,  $18.9^\circ$  and  $32.1^\circ$ .

Example 2. A radial cam rotates clockwise, with  $R = 60$  mm,  $\varepsilon = -15$  mm. Figure 14 shows its displacement motion; we have the following sections: AB - Rise; BC - Constant velocity; CD - Rise; DE - Dwell; EF - Return; FG - Dwell. Motion curves chosen for sections AB, CD and EF are C-1, C-2 and C-6, respectively.

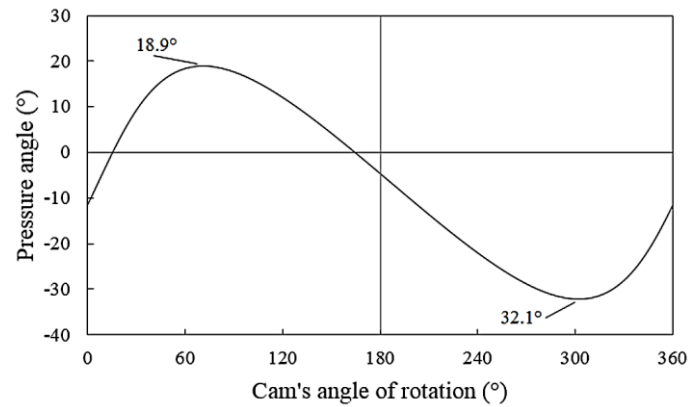


Figure 13. Pressure angle for cam full rotation of Example 1.

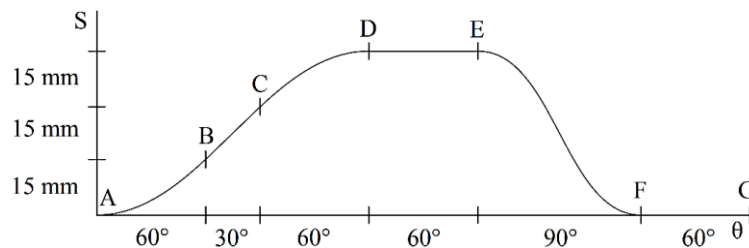


Figure 14. Displacement curve for Example 2.

For section AB, since it is a half-curve, we have to use the relations given in Equations (26) to (30). We have  $L_1 = 30$  mm,  $\beta_1 = 120^\circ$ . Thus  $L/R = 0.5$  and  $\varepsilon/R = -0.25$ . By looking at the left side of Figure 10, we find  $B = 1.37$ . Using this answer on the right side, we get an approximate maximum pressure angle  $\alpha_{\max} = 31.0^\circ$ .

For section CD, we have to use the same relations, however base radius needs to take into account the follower rise so far before calculating the new base radius. Thus,  $L_1 = 30$  mm;  $R_0 = 90$  mm,  $R_1 = 75$  mm. Then, we have  $L/R = 0.4$ ;  $\varepsilon/R = -0.2$  and  $\beta = 120^\circ$ . Through Figure 10, we find  $B = 1.41$  and an approximate  $\alpha_{\max} = 26.0^\circ$ .

Finally, for section EF, we can use the unchanged values of base radius and active cam angle and, since it is a return motion, we use a positive value of eccentricity. Thus we have  $L/R = 0.75$ ;  $\varepsilon/R = +0.25$  and  $\beta = 90^\circ$ . Through Figure 10, we find  $B = 1.43$  and an approximate  $\alpha_{\max} = 29.0^\circ$ .

Plotting Equation (1) with these parameters, Figure 15 shows that the maximum pressure angles for sections AB, CD and EF are, respectively,  $31.5^\circ$ ,  $26.4^\circ$  and  $28.3^\circ$ .

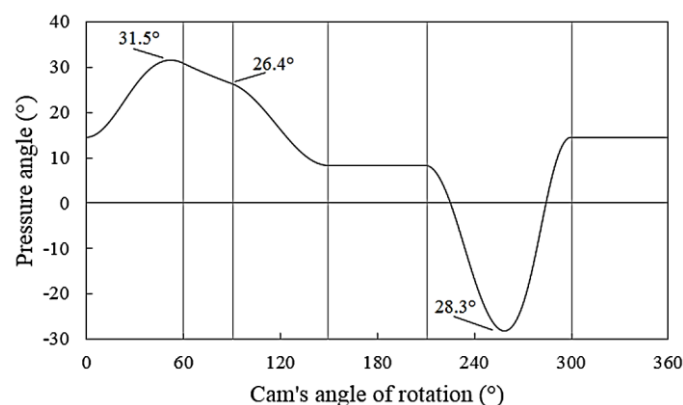


Figure 15. Pressure angle for cam full rotation of Example 2.

### Advantages and tips for using nomograms

Nomograms have the advantage of providing a visual aid in which parameters can be modified in cases where the maximum pressure angle is above  $30^\circ$ . Figures 10 and 11 show that high values of  $B$  give greater chances of obtaining a small value for  $\alpha_{\max}$ , since high values of active cam angle are rare. In order to achieve high values of  $B$ , we should have low ratios of  $L/R$  along with low values of  $\varepsilon/R$ . For higher ratios of  $L/R$ , a higher eccentricity can help in finding higher values for  $B$ .

One can also easily manipulate values for stroke, radius and eccentricity during cam design to achieve lower pressure angles. Increasing base radius reduces  $L/R$  and  $\varepsilon/R$  ratios, reducing the maximum pressure angle value. Also, a change in eccentricity may be easier to perform on an operating machine, the nomograms help to quickly quantify that change and avoid trial and error.

A change in active cam angle is also possible, but extra care has to be taken when using given charts, since  $\beta$  appears on the left and right side of the chart. Both can be changed at the same time, or one at a time iteratively, depending on whether other parameters must remain the same.

## Conclusion

Radial cams with translating followers have the limitation of having a maximum pressure angle of up to  $30^\circ$ , which is a complex problem to be solved in cam design. A simple solution to manipulate this angle is by using the eccentricity between the axes of the follower and cam, which is usually done by trial and error. Nomograms have the advantages of being simple and quick to apply, in addition to being a graphical representation of the problem as a whole, providing insight into the relationship of the input parameters. The charts given here assist in using stroke, base radius, active cam angle and eccentricity parameters together to obtain maximum pressure angles according to necessary conditions. Up until now, no nomograms with so many parameters have been available. Although several recent methodologies for controlling maximum pressure angle provide precise answers, it is common the need to return to the drawing board to modify parameters to adapt to a larger engineering project. Since a nomogram is a printed chart, by utilizing a straight line it is possible to alter this variable and keep others intact and check in a matter of seconds how the maximum pressure angle changes. The use of nomograms is by no means a substitute for other ways of designing cams with low pressure angles, but a simple and quick form of calculation that may be sufficient for a project, serve as a guide and a starting point for a more optimized project or even find usefulness on undergraduate level textbooks.

## Supplementary material

The final nomograms for cycloidal and harmonic curves are given as supplementary material in high quality. Additionally, the codes to create the nomograms are also available; in order to run them, it is necessary to install the PyNomo package for Python.

## Acknowledgements

The authors would like to acknowledge Dr. Leif Roschier for creating the PyNomo package for Python and help on the usage.

## References

- Ambekar, A. G. (2007). *Mechanism and machine theory*. New Delhi, ID: Prentice Hall.
- Bagaria, W. J., Doerfler, R., & Roschier, L. (2017). Nomograms for the design of light weight hollow helical springs. *Proceedings of the Institution of Mechanical Engineers, Part C: Journal of Mechanical Engineering Science*, 231(23), 4388-4394. DOI: <https://doi.org/10.1177/0954406216665416>
- Dicker, J. J., Pennock, G. R., & Shigley J. E. (2003). *Theory of machines and mechanisms*. New York, NY: Oxford University Press.
- Doerfler R. (2009). The lost art of nomography. *The UMAP Journal*, 30(4), 457-493.
- Epstein, L. I. (1958). *Nomography*. New York, NY: Interscience.
- Esmail, E. L., Pennestrib, E., & Juber A. H. (2018). Power losses in two-degrees-of-freedom planetary gear trains: A critical analysis of Radzimovsky's formulas. *Mechanism and Machine Theory*, 128, 191-204. DOI: <https://doi.org/10.1016/j.mechmachtheory.2018.05.015>
- Farouki, R. T., & Manjunathaiah, J. (1998). Design of rational cam profiles with Pythagorean-hodograph curves. *Mechanism and Machine Theory*, 33(6), 669-682. DOI: [https://doi.org/10.1016/S0094-114X\(97\)00099-2](https://doi.org/10.1016/S0094-114X(97)00099-2)
- Flores P. (2013). A computational approach for cam size optimization of disc cam follower mechanisms with translating roller followers. *Journal of Mechanisms and Robotics*, 5(4), 041010-041016. DOI: <https://doi.org/10.1115/1.4025026>

- Hwang, W., & Chen, K. (2007) Triangular nomograms for symmetrical spherical non-Grashof double-rockers generating symmetrical coupler curves. *Mechanism and Machine Theory*, 42(7), 871-888. DOI: <https://doi.org/10.1016/j.mechmachtheory.2006.05.008>
- Jensen, P. W. (1987). *Cam design and manufacture*. New York, NY: Marcel Dekker.
- Kloomok, M., & Muffley, R. V. (1955). Plate cam design: Pressure angle analysis. *Product Engineering*, 26,155-160.
- Ma, Z., Chong, H. Y., & Liao, P. (2020). Real-time safety inspection and planning: A first application of the Fagan nomogram. *Canadian Journal of Civil Engineering*, 47(4),438-449. DOI: <https://doi.org/10.1139/cjce-2018-0500>
- Mabie, H. H., & Reinholtz, C. F. (1987). *Mechanisms and dynamics of machinery*. New York, NY: John Wiley & Sons.
- Norton, R. L. (2009). *Cam design and manufacturing handbook*. New York, NY: Industrial Press.
- Norton, R. L. (2012). *Kinematics and design of machinery*. New York, NY: McGraw-Hill.
- Rao, J. S. (2011). *Kinematics of machinery through HyperWorks*. New York, NY: Springer.
- Rothbart, H. A. (2004). *Cam design handbook*. Teaneck, NJ: McGraw-Hill.
- Suchora, D. H., Werner, B. C., & Paine, W. A. (1994). Pressure angle characteristics of radial cams with offset reciprocating roller follower. In *Proceedings of the ASME 1994 Design Technical Conferences collocated with the ASME 1994 International Computers in Engineering Conference and Exhibition and the ASME 1994 8th Annual Database Symposium. 23rd Biennial Mechanisms Conference: Machine Elements and Machine Dynamics* (p. 103-114). Minneapolis, MN: ASME. DOI: <https://doi.org/10.1115/DETC1994-0248>
- Varnum, E. C. (1951) Circular nomogram theory and construction technique. *Product Engineering*, 22, 152-156.
- Yu, Q., & Lee, H. P. (1998). Size optimization of cam mechanisms with translating roller followers. *Proceedings of the Institution of Mechanical Engineers, Part C: Journal of Mechanical Engineering Science*, 212(5),381-386. DOI: <https://doi.org/10.1243/0954406981521303>